# Multi-Joint Leg Moment Estimation During Walking Using Thigh or Shank Angles

Mahdy Eslamy and Mo Rastgaar, *Senior Member, IEEE*

***Abstract*— To reinstate human-like locomotion by using robotic prosthetics, orthotics or exoskeletons, a main challenge is how to coordinate the motion of these devices with that of the biological limbs. One approach to overcome this challenge is to identify firstly the relationships that exist between the kinematics and kinetics of the lower extremity joints and limbs. In this work we aimed to continuously estimate sagittal plane ankle, knee and hip moments using shank or thigh angles. For this purpose, neural network and wavelets were used in a nonlinear auto-regressive model with exogenous inputs. This approach circumvented the need for switching rules or intermediate parameters. To assess the performance of the estimator, four case studies were developed. First, thigh angles (inputs) were used to estimate hip moments (outputs). Second, thigh angles were used to estimate knee moments. Third, ankle moments were estimated using thigh angles, and in the fourth case study, ankle moments were estimated using shank angles. Three different databases involving 106 subjects at different walking speeds were used to evaluate estimation quality. The testing procedure involved both inter-subject and intra-subject evaluations. The best estimation performance was observed when ankle moments were estimated from shank angles. The weakest estimation performance was observed when knee moments were estimated using thigh angles at 0.5 m/s. For this case, the estimation quality was much better at 1.5 m/s. Average RMS errors were 0.13 – 0.15, 0.10 – 0.13, and 0.09 – 0.12 [Nm/kg] for hip, knee and ankle moments, respectively. Average mean absolute errors MAEs were 0.10 – 0.11, 0.07 – 0.10, and 0.06 – 0.08 [Nm/kg] for hip, knee and ankle moments, respectively. Average correlation coefficients were 0.90 – 0.98 and 0.98 – 0.99 for hip and ankle moment estimations. The value for knee was comparable only at high speed (0.96 for 1.5 m/s), while it was less accurate at slow speed (0.71 for 0.5 m/s). In general, for all of the joints, the estimation accuracy was comparable with that of other studies, although one source of input was employed (either shank or thigh angle).**

***Index Terms*— Estimation of leg moments, prosthetics, orthotics, motion planning.**

## I. Introduction

TO DEVELOP high-level controllers and motion planners for intelligent assistive devices such as robotic orthotics, prosthetics, and exoskeletons [1], [2], [3], [4], and gait rehabilitation devices [5], [6], one approach is to create relationships between gait variables such as joints' kinetics and kinematics, muscular activities and/or ground reaction forces.

To estimate joints' moments, different algorithms have been suggested in which a wide range of inputs such as gait kinematics, kinetics, EMG (electromyography) signals, demographic (e.g., age and gender) and anthropometric (e.g., height and mass) information were used.

Some studies used impedance concept to express ankle and knee moments as a function of joint's angular positions and velocities multiplied by stiffness and damping gains [2], [3], [4], [7], [8], [9]. These algorithms are sometimes used with finite-state machine approach, in which a gait cycle is segmented into different phases (states) (e.g., into four [2]). For each state, stiffness and damping gains were determined piece-wise, first based on average human gait data, e.g., from [10] and then tuned based on subject-specific experimental data. Next, the gains were obtained using a constrained least-squares optimization for each state [2]. Both linear [3] and nonlinear [2], [11], [12] expressions were proposed to represent knee/ankle moments. In addition to the gait cycle segmentation, another requirement was defining some switching rules to transit between different gait phases.

To avoid gait cycle segmentation, the impedance approach was combined with other algorithms. In [13], LASSO regression (least absolute shrinkage and selection operator) was utilized to predict ankle, knee, and hip moments as a linear summation of stiffness and damping gains multiplied by joint angular positions and velocities, respectively. To estimate, e.g., ankle moment, the method however required ankle, knee and hip angles and angular velocities from both ipsi- and contra-lateral sides. In [14], in addition to angular and angular velocity terms, angular acceleration and gravity terms were included to estimate the hip moment. This approach was limited to a specific walking speed.

The phase plane approach was proposed in [14] to continuously predict ankle motions during walking. The method required gait percents and walking speeds to estimate the corresponding motions. To estimate those parameters, shank angular velocities and angles were employed as inputs. Next, the corresponding ankle moments or angles were found out using a previously produced off-line look-up table. To predict different speeds, conditional if-then statements were also required. A Gaussian process regression algorithm was developed in [15] to predict ankle moments for twenty-one subjects using shank angular positions and velocities. In that approach,

Manuscript received 15 April 2022; revised 27 September 2022; accepted 23 October 2022. Date of publication 26 October 2022; date of current version 6 February 2023. This work was supported by the National Science Foundation (NSF) under Grant 1921046. *(Corresponding author: Mahdy Eslamy.)*

Mahdy Eslamy is with the School of Computing, Engineering and Digital Technologies, Teesside University, TS1 3BX Middlesbrough, U.K. (e-mail: m.eslamyatgmail.com).

Mo Rastgaar is with the Purdue Polytechnic Institute, Purdue University, West Lafayette, IN 47907 USA.

Digital Object Identifier 10.1109/TNSRE.2022.3217680

This work is licensed under a Creative Commons Attribution 4.0 License. For more information, see https://creativecommons.org/licenses/by/4.0/

it was not necessary to predict speeds or gait percents. Instead, the inputs were directly mapped to the outputs without requiring those intermediate parameters.

In [16], hip angles together with thigh Euler angles were processed in an artificial neural network to estimate the corresponding gait percents. A cosine function (with gait percents as inputs) was then used to simplistically represent the hip moments. The work was later continued in [17], where two machine learning algorithms (extreme gradient boosting algorithm and a feed-forward neural network) were implemented to estimate subject-specific hip moments. To perform moment estimations, hip angles, gyroscopic data and six-axis acceleration from a thigh-mounted IMU were used. The study concluded that both methods had relatively similar estimation quality.

Electromyography (EMG) signals are the other types of the inputs used for moment estimation [18], [19], [20], [21]. In [22], a neural network was utilized to estimate ankle moments for very slow to fast walking speeds. EMG signals obtained from five lower extremity muscles were used for this purpose. The study showed that EMG signals extracted from tibialis anterior, medial gastrocnemius and biceps femoris (combined) led to the lowest root mean square errors. On the other side, EMG signals from tibialis anterior and medial gastrocnemius (combined) led to very slightly less favorable results.

In [23], ground reaction forces together with EMG signals were used to continuously estimate ankle, knee and hip moments during walking. Performance of a wavelet neural network was compared with that of a feed forward neural network for four subjects. Results showed that the wavelet approach could predict joint moments with higher accuracy, however, the method required a high number of inputs (two ground reaction forces and eight EMG signals). Different studies reported that merging kinematics with EMG inputs can lead to better estimation accuracy in comparison to solely using EMG signals, [24], [25], [26], [27].

In addition to EMG and kinematics data, anthropometrics and demographics are also used as inputs to different algorithms. An artificial neural network with three layers was designed in [28] to convert various inputs (kinematics, anthropometrics, demographics, electromyography) to the sagittal plane ankle, knee and hip moments during self-selected walking for nineteen healthy young subjects.

Interestingly, the study showed that using less inputs including only kinematics (joint angles, velocities and accelerations) and demographics (age and gender) led to a relatively similar estimation quality compared to using a complete set of the inputs. Furthermore, the study reported that the estimation performance using EMG plus demographics inputs was less accurate than the kinematics plus demographics inputs.

In [29], hip, knee and ankle angles together with gait velocity, subjects' height and weight, and foot, shank and thigh lengths were used to estimate lower extremity joints' moments. To do so, an artificial neural network was trained with inputs from twelve subjects walking from 0.8 to 2 m/s. The work was later continued in [30], in which the angular velocities and linear accelerations of the lower extremity limbs were used to estimate ankle, knee and hip moments during walking (only stance phase). The performance of two algorithms, a long short term memory neural network and a feed forward one was compared. Both approaches had relatively similar results.

A customized instrumented insole and a tissue force sensor were developed in [31] to estimate ankle moments for six healthy subjects. An artificial neural network was developed to compare the estimated values with those obtained from an inverse dynamics procedure. The effects of different inputs (ankle angles, inputs from instrumented insole, Achilles tendon force) were investigated on the estimation results.

State estimation with minimal inputs is of interest in biomechanical gait analysis or designing control algorithms for assistive devices, [22], [28], [32], [33]. This potentially leads to robotic assistive devices with less embedded sensors (and markers, in case of gait studies).

In this work, we focus on the estimation of the sagittal plane ankle, knee and hip moments using only thigh or shank angles, depending on the joint under investigation. The target is to estimate joint moments using minimal sensory information which can be potentially obtained from a lower limb proximally above a specific joint. For instance, when possible (e.g., for knee and ankle joints), estimation was performed using the lower limb's angle above the respective joint (thigh angle for knee moment estimation, or shank angle for ankle moment estimation). The reason is that we would like to develop a motion planner whose outputs are a function of relatively independent inputs. Obtaining inputs from a lower limb which is below a specific joint, will result in a motion planner whose inputs are directly influenced by the movement of the corresponding joint, and hence creates a paradoxical situation for the motion planner. Therefore, we used the logical hierarchy existing in the human body structure.

Furthermore, it was aimed to eliminate the need for speed or gait percent identification, switching rules or look-up tables. To achieve these targets, a nonlinear auto-regressive model was used in combination with wavelets and neural networks to estimate those variables.

We used this approach previously to estimate ankle and knee angles for several walking speeds [34]. In this study, this algorithm is extended to multi-joint moment estimation for lower extremities. This helps us create a potential comprehensive and integrated controller and motion planner to be used in robotic prostheses or orthoses.

The human gait has periodic as well as variable nature. Similar to Fourier series, the wavelets theory [35] expresses a function (a signal) as the sum of a series of weighted small waves called wavelets. The wavelets rise and decay through time, and therefore have a fundamental difference with basis functions used in Fourier series. Therefore, the wavelets can chase the changes of system response both in time and frequency domains [36], [37], [38], and as a result can describe a part of a function with a resolution corresponding to its scale. Further discussion is presented in the Methods section.

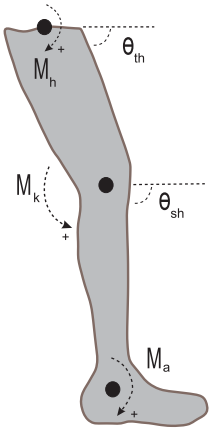


Fig. 1. Definition of the thigh and shank angles $\theta_{th}$, $\theta_{sh}$, together with hip, knee and ankle moments $M_h$, $M_k$, $M_a$.

## II. Methods

Shank or thigh angles were used to estimate sagittal plane ankle, knee and hip moments. For this purpose, three databases involving 106 subjects were used.

The first database was obtained from [39], in which twenty-one subjects (1.73±0.09 m, 70.9±11.7 kg, 25.4±2.7 yr) walked at slow, moderate and fast speeds (0.5, 1, and 1.5 m/s). The second database (publicly available) was obtained from [40], in which thirty-seven subjects walked at eight different (subject-specific) speeds (young adults (27.6±4.4 yr, 171.1±10.5 cm, 68.4±12.2 kg) and older adults (62.7±8.0 yr, 161.8±9.5 cm, 66.9±10.1 kg)). The third database (publicly available) was obtained from [41], in which forty-eight subjects walked at several speeds (6 – 72 yr, 18.2 – 110 kg, 116.6 – 187.5 cm). In the second and third databases, each subject walked at self-selected speeds which were not necessarily similar to another participant's speeds. Therefore, unlike the first database, the participants were not required to walk at fixed specific speeds.

The definitions of thigh angle $\theta_{th}$, shank angle $\theta_{sh}$, hip moment $M_h$, knee moment $M_k$ and ankle moment $M_a$ are shown in Fig. 1. In Fig. 2A-E, hip, knee and ankle moments as well as thigh and shank angles, are shown for twenty-one subjects together with their mean curves. The numerical values in Fig. 2 were obtained from [39].

To estimate joints' moments, a nonlinear autoregressive model with exogenous inputs (NARX) [42] was developed. We previously used this modeling approach to estimate joints' angles for different speeds [34]. The proposed model is comprised of the inputs, the estimator and the outputs Fig. 3. The outputs are the estimated joints' moments $\hat{y}$ (e.g., $\hat{M}_h$). In this algorithm, the inputs consist of the current and past values of the external inputs $u$ (thigh or shank angles) and past values of the estimated outputs $\hat{y}$ (hip/knee/ankle moments). The estimator $\hat{f}$, creates a functional relationship between the outputs and the inputs. According to the above, we will have

$$\begin{aligned} \hat{y}(k) &= \hat{f}(x(k)) \\ x(k) &= [\ldots, \hat{y}(k-1), u(k), u(k-1), \ldots] \end{aligned} \tag{1}$$

The dimension $d$ of the $x$ is usually determined according to the problem to be solved [25], [43], [44], [45]. Having the

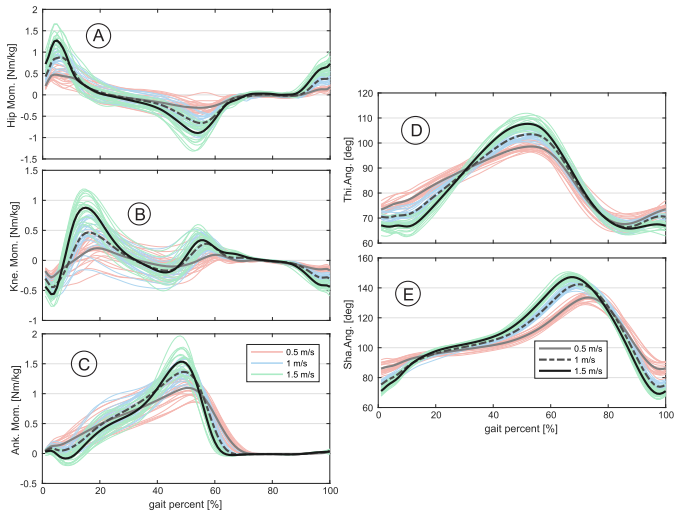


Fig. 2. The curves of (A): hip moments $M_h$, (B): knee moments $M_k$, (C): ankle moments $M_a$, (D): thigh angles $\theta_{th}$ and (E): shank angles $\theta_{sh}$ (twenty-one subjects walking at 0.5, 1 and 1.5 m/s). For each speed, the mean curves are in bold. The numerical values were obtained from the first database [39].

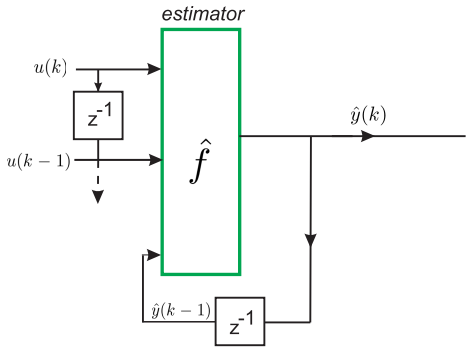


Fig. 3. The schematic view of the estimation algorithm, the figure shows the input at time instant $k$ for the case $x(k) = [\hat{y}(k-1), u(k), u(k-1)]$. The estimator $\hat{f}(x(k))$ then processes the input to produce the estimated outputs $\hat{y}(k)$.

above definitions in mind, the estimation algorithm works as depicted in Fig. 3.

To define estimator $\hat{f}$, wavelets [36], [37], [38] have been used. In general, to enhance the estimation quality, a summation of the wavelets in the form of a network is used [46], [47]. The wavelets theory is similar to the Fourier series. The main difference is that wavelets can describe a function more accurately when its frequency changes with respect to time (which is common in human gait) or when singularities happen at some region of a function.

Wavelets theory converts a signal into small waves (i.e., the wavelets). Unlike basis functions of the Fourier series (sine and cosine functions), the basis function of the wavelets theory grow and decay through time. According to above, the estimator $\hat{f}$ can be written as $\hat{f}(x) = \Sigma_{i=1}^{L} \omega_i \psi_i(x)$.

Different options exist for the basis function $\psi(x)$. In this study, the Gaussian derivatives family [48] was selected which is usually used to study joints' motions [49], [50], [51], [52], [53]. Therefore, $\psi(x) = (d - xx^T)e^{-\frac{xx^T}{2}}$. In the above equations, $L$ is the number of wavelets, $x^T$ denotes the

transpose of $x$ and $d$ is the dimension of the input $x$ [35], [36], [37], [38], [48].

The definition of $\hat{f}$ shows that wavelets can be combined with neural networks theory. The input of the network would be according to $[x(k)]$, and the hidden layer of the network contains the wavelets-based basis functions together with the $\omega$ coefficients. Finally, the outputs are the estimated joints' moments. Further information about wavelets can be found in [35], [36], [37], [46], [47], [48], and [38]. In addition, more details are provided in [34].

To estimate joint moments, four case studies were designed: **1**) hip moments $M_h$ (estimated outputs $\hat{y}$) were estimated using thigh angles $\theta_{th}$ (external inputs $u$), **2**) knee moments $M_k$ were estimated using thigh angles, **3**) ankle moments $M_a$ were estimated using thigh angles, and **4**) ankle moments $M_a$ were estimated using shank angles $\theta_{sh}$.

To train and test the algorithm, different approaches were adopted to evaluate the performance. For the first database [39], the leave-one-subject-out cross validations was used. Therefore, for each case study explained above, the inputs from twenty participants were used for training. Next, the inputs from one remaining subject was used for testing. This procedure was carried out for each individual to estimate the corresponding joints' moments.

The participants in the second and third databases, walked at different speeds individually. For the second database [40], for each subject, data from three speeds were used for training, and data from the remaining five speeds of that subject were used for testing the estimation performance (intra-subject). For the third database [41], depending on the available data, for some subjects more than five speeds and for some less than five were used for testing the estimation performance (intra-subject).

According to Fig. 3, the external input $u$ is $\theta_{th}$ or $\theta_{sh}$, and the estimated output $\hat{y}$ is $\hat{M}_h$, $\hat{M}_k$ or $\hat{M}_a$, depending on the joint under study. The root mean square (RMS) errors, the mean absolute errors (MAEs), and the correlation coefficient [19], [54], [55] were used to evaluate the estimation quality of the four case studies defined above.

$$RMSE = \sqrt{\frac{\sum_{i=1}^{n}(M_i - \hat{M}_i)^2}{n}}$$
$$MAE = \frac{\sum_{i=1}^{n}|M_i - \hat{M}_i|}{n}$$
$$\rho_{cc} = \frac{\sum_{i=1}^{n}(M_i - \bar{M})(\hat{M}_i - \bar{\hat{M}})}{\sqrt{\sum_{i=1}^{n}(M_i - \bar{M})^2}\sqrt{\sum_{i=1}^{n}(\hat{M}_i - \bar{\hat{M}})^2}} \quad (2)$$

In the formulas above, $n$ is the number of the samples, $\hat{M}$ is the estimated moment, and $M$ is the actual one.

Since activation functions of the algorithm are of the wavelets form, it is a nonlinear auto-regressive model. In the linear version, $\hat{f}$ is expressed as a linear combination of the past and current external inputs and past outputs. This version would then be of the form $\hat{f}(x(k)) = a_0u(k)+a_1u(k-1)+\ldots+b_1\hat{y}(k-1)+\ldots$, in which $a_i$'s and $b_i$'s are scalar values. The estimation results of both linear and nonlinear versions are compared in this study (section III-A).

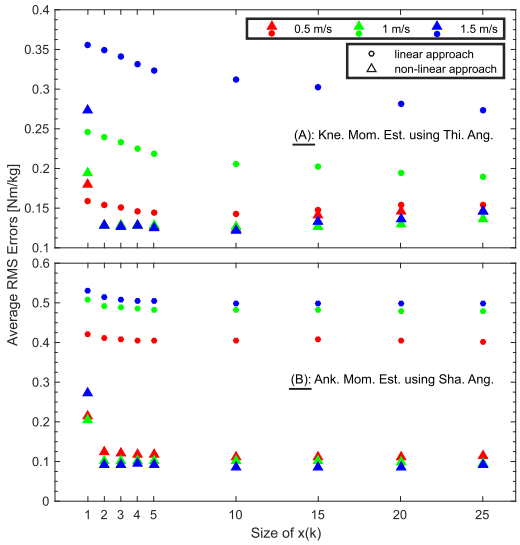


Fig. 4. (Subsection III-A) Comparison between the average RMS errors in nonlinear and linear models with respect to size of $x(k)$. (A): knee moment estimations using thigh angles, and (B): ankle moment estimations using shank angles. The values are for the subjects of the first database [39] at different speeds.

According to the definition of $x(k)$, it can contain different components. It was of interest to keep the number of the components to a minimum level. Therefore, the performance of the estimator $\hat{f}$ was evaluated according to different components of $x(k)$ (sections III-A and III-B) to find out the optimal size of $x$. To decouple the influence of the past estimations on the new ones, the inclusion of the past outputs in $x(k)$ was avoided. Therefore, the estimation of the joints' moments got dependent only on the *external* inputs $u$ originated from a lower limb (shank or thigh). Nevertheless, the impact of the inclusion of the past estimations on the performance of the algorithm is investigated later in this study. The results are discussed in the next section.

## III. Results

### A. Linear vs. Nonlinear Auto-Regressive Model

Fig. 4A-B compares the performance of a linear model vs. a nonlinear one. It shows the mean RMS errors of the knee and ankle moment estimations using thigh and shank angles, respectively. Those mean values are for the the participants of the first database [39] at different speeds. Furthermore, the figure shows the variations of the RMS errors with respect to different sizes of input $x(k)$.

Fig. 4A-B shows that for all of the speeds, the RMS errors of the linear model were much higher than those of the corresponding nonlinear model (excluding $x(k) = [u(k)]$). According to the observed RMS errors, the non-linear model was preferred. Fig. 4A-B also shows that the RMS errors in the non-linear model, tend to their minimums faster than the linear one. Fig. 4 shows that increasing the dimension of input $x(k)$ does not necessarily lead to better estimation.

### B. Impact of the Input Size on the Estimation (in Nonlinear Model)

Fig. 5A-D shows the variation of the average RMS errors of the nonlinear model with respect to different sizes of $x(k)$. The

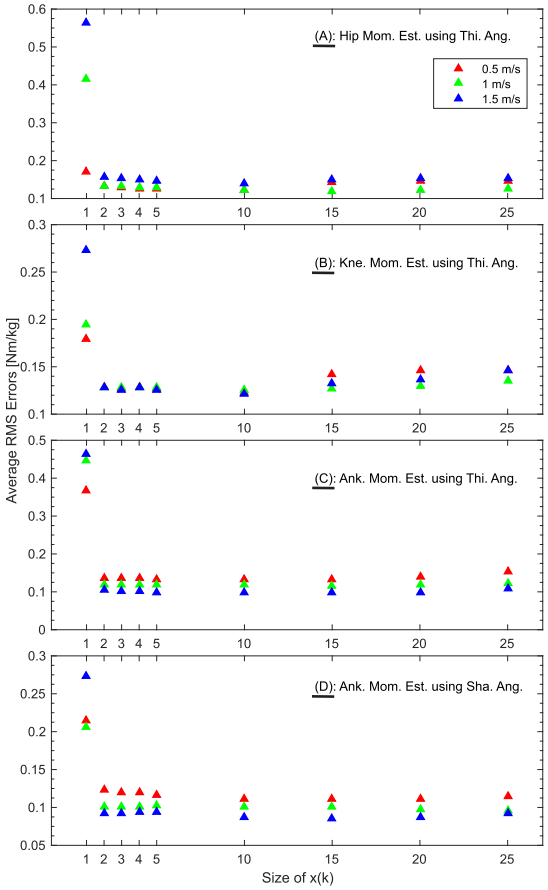


Fig. 5. (Subsection III-B) The change of average RMS errors for the nonlinear model with respect to different sizes of $x(k)$. Figures A-D are according to the four case studies explained in the Methods section. The average values are for the subjects of the first database [39] at various speeds.

average values are for the subjects of the first database [39] at different speeds and according to the four case studies explained in the Methods section.

In Fig. 5A, when $x(k) = [u(k)]$ (i.e., size of $x(k)$ is 1), the average RMS errors were high. The values declined considerably when $x(k) = [u(k), u(k-1)]$, for all of the speeds. This trend is seen in sub-figures B to D as well. Fig. 5A also shows that increasing the dimension of $x(k)$ does not necessarily lead to a continuous decline of the average RMS errors. This is especially more visible in Fig. 5B-D.

Therefore, using Fig. 5A-D, the size of the $x(k)$ was decided based on the trade-off (compromise) between complexity of $x(k)$ (i.e., its size) and RMS errors at different speeds. Thus, for the first database [39], for case study 1 the size of $x(k)$ was set to 5 (i.e., $x(k) = [u(k), \ldots, u(k-4)]$), for case study 2 the size of $x(k)$ was set to 3, for case study 3 the size of $x(k)$ was set to 5, and for case study 4 the size of $x(k)$ was set to 4. It should be noted that, for instance, for case study 1, Fig. 5A shows that when size of $x(k)$ is 10, the minimum results are obtained, however in comparison to the compromised input size (i.e., 5, as we discussed before), the differences were not very considerable. For this case, the RMSE decrease was 3.9%, 4.2%, and 5.2% for 0.5, 1 and 1.5 m/s, respectively (selected vs. minimum). According to the above, we decided to reach a compromise between computational costs due to the size of the input, and RMS errors. Furthermore, it was of interest to avoid the reliance of the current output to too many previous inputs, since it might result in improper response of the motorized prosthetics/orthotics in real-world applications. Therefore, we took into consideration a spectrum of objectives and their impacts/importance. This attitude was adopted throughout this work for each case study. For the second [40] and third [41] databases, the size of $x(k)$ is reported at the corresponding Results subsections.

### C. RMS Errors, MAEs and $\rho_{cc}$ for First Database [39]

Fig. 6 shows the root mean square (RMS) errors (A), mean absolute errors (MAEs) (B), and $\rho_{cc}$ values (C) for different subjects and speeds (first database [39]). For better comparison, the results are also reported in Tab. I.

The cyan circles are for the first case study, where thigh angles $\theta_{th}$ were used to estimate hip moments $M_h$. The blue circles are for the second case study, where thigh angles $\theta_{th}$ were used to estimate knee moments $M_k$. The red circles show the results for the third case study, where thigh angles $\theta_{th}$ were used to estimate ankle moments $M_a$, and the green circles are for the fourth case study, where shank angles $\theta_{sh}$ were used to estimate ankle moments $M_a$. The black squares denote the mean values in each case study. All of the values mentioned in this subsection are for 0.5 m/s, 1 m/s and 1.5 m/s, respectively.

*1) Estimating Hip Moment Using Thigh Angles:* The average±std RMS errors were 0.13±0.05, 0.13±0.05 and 0.15±0.05 [Nm/kg] (0.5 m/s, 1 m/s and 1.5 m/s, respectively). The average mean absolute errors (MAEs) errors were 0.10±0.04, 0.10±0.04 and 0.11±0.04 [Nm/kg]. The average $\rho_{cc}$ were 0.90±0.09, 0.97±0.02 and 0.98±0.01.

*2) Estimating Knee Moment Using Thigh Angles:* The average±std RMS errors were 0.13±0.05, 0.13±0.06 and 0.13±0.06 [Nm/kg]. The MAEs errors were 0.10±0.04, 0.10±0.05 and 0.09±0.05 [Nm/kg]. The average $\rho_{cc}$ were 0.71±0.20, 0.90±0.13 and 0.96±0.03.

*3) Estimating Ankle Moment Using Thigh Angles:* The average RMS errors were 0.13±0.05, 0.12±0.04 and 0.10±0.04 [Nm/kg]. The MAEs errors were 0.10±0.04, 0.08±0.02 and 0.07±0.03 [Nm/kg]. The average $\rho_{cc}$ were 0.96±0.04, 0.98±0.01 and 0.98±0.01.

*4) Estimating Ankle Moment Using Shank Angles:* The average RMS errors were 0.12±0.05, 0.10±0.04 and 0.09±0.03 [Nm/kg]. The MAEs errors were 0.08±0.04, 0.07±0.03 and 0.06±0.02 [Nm/kg]. The average $\rho_{cc}$ were 0.98±0.02, 0.99±0.01 and 0.99±0.01.

### D. Ankle, Knee and Hip Moments: Estimated vs. Gait Data

Fig. 7A-D compares the estimated ankle, knee and hip moments versus gait data for several speeds and subjects (related to the first database [39]), according to the four case studies explained in the Methods section. Fig. 7A (first column) is related to estimating the hip moment (case study 1). The second column (Fig. 7B) is related to estimating the knee

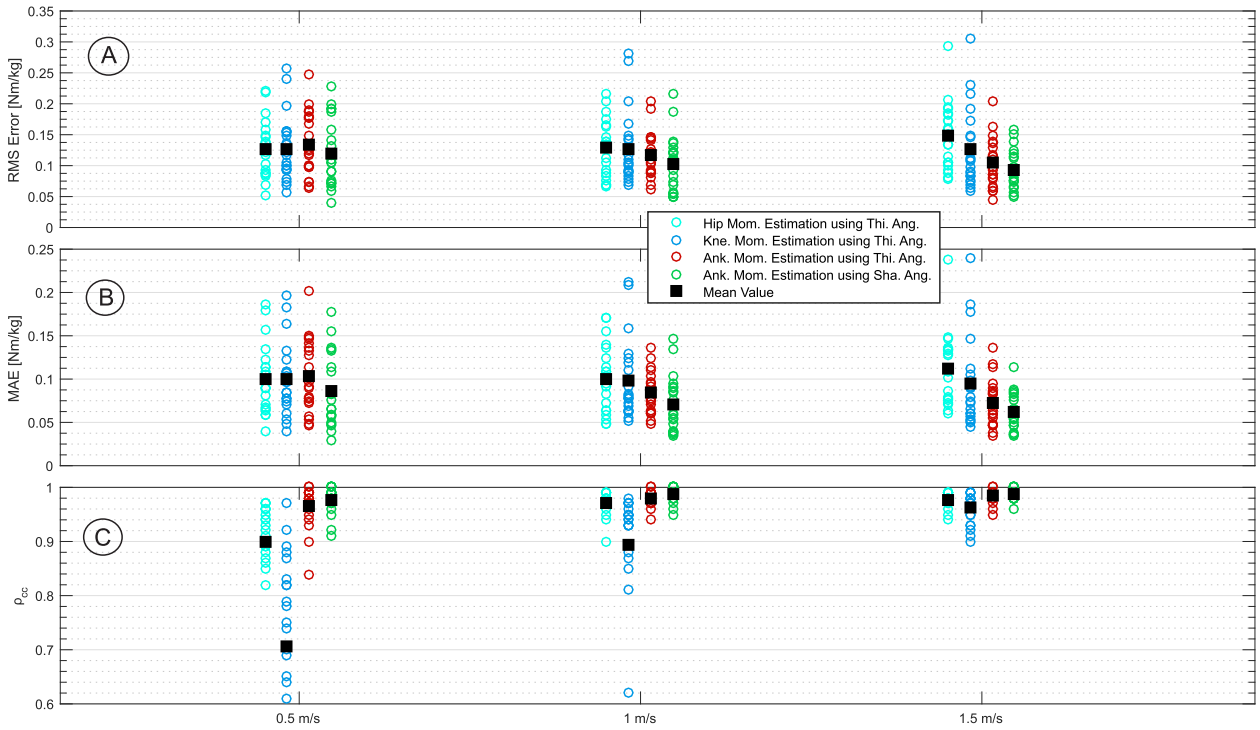


Fig. 6. (Subsection III-C) The root mean square (RMS) errors (A), mean absolute errors (MAEs) (B) and $\rho_{cc}$ (C) values for hip, knee and ankle moment estimations for different inputs ($\theta_{th}$ or $\theta_{sh}$), speeds and subjects (first database [39]), according to the four case studies explained in the Methods section. For each case study the mean values are indicated by the black squares.

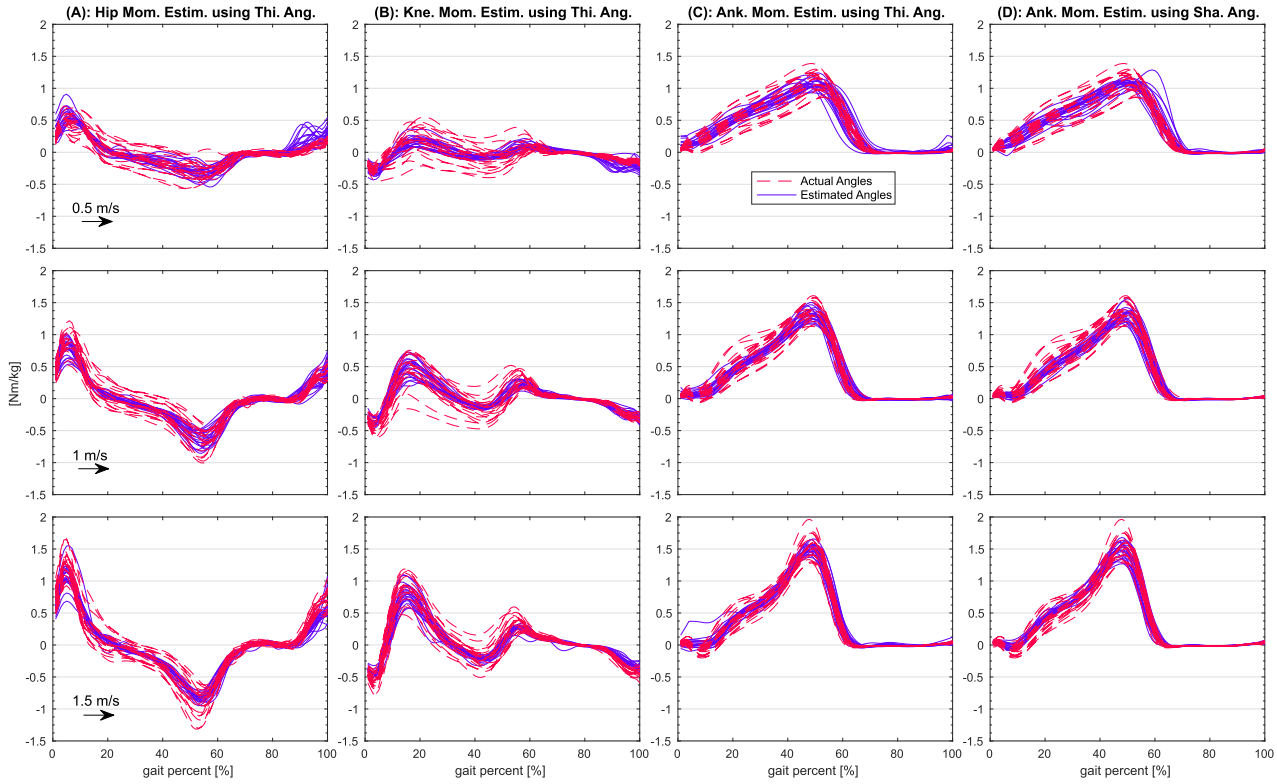


Fig. 7. (Subsection III-D) The estimated hip, knee and ankle moments vs. gait data for various speeds and subjects (first database [39]), according to the four case studies explained in the Methods section.

moment (case study 2). The third column is related to the ankle moment estimations using thigh angles (case study 3), and the fourth column is related to the ankle moment estimations using shank angles (case study 4).

For the first database, since all of the participants performed experiments at specific speeds, it was possible for us to provide the figures (Fig. 6 and Fig. 7) and the results, grouped based on the speeds.

TABLE I
COMPARISON OF AVERAGE(±STD) RMS ERRORS, MAES AND $\rho_{cc}$ (DATABASE 1, SEE ALSO SUBSECTION III-C)[2]

| | $M_h(\theta_{th})$[1] | | | $M_k(\theta_{th})$ | | | $M_a(\theta_{th})$ | | | $M_a(\theta_{sh})$ | | |
|---|---|---|---|---|---|---|---|---|---|---|---|---|
| | 0.5 m/s | 1.0 | 1.5 | 0.5 | 1.0 | 1.5 | 0.5 | 1.0 | 1.5 | 0.5 | 1.0 | 1.5 |
| RMSE | 0.13±0.05 | 0.13±0.05 | 0.15±0.05 | 0.13±0.05 | 0.13±0.06 | 0.13±0.06 | 0.13±0.05 | 0.12±0.04 | 0.10±0.04 | 0.12±0.05 | 0.10±0.04 | 0.09±0.03 |
| MAE | 0.10±0.04 | 0.10±0.04 | 0.11±0.04 | 0.10±0.04 | 0.10±0.05 | 0.09±0.05 | 0.10±0.04 | 0.08±0.02 | 0.07±0.03 | 0.08±0.04 | 0.07±0.03 | 0.06±0.02 |
| $\rho_{cc}$ | 0.90±0.09 | 0.97±0.02 | 0.98±0.01 | 0.71±0.20 | 0.90±0.13 | 0.96±0.03 | 0.96±0.04 | 0.98±0.01 | 0.98±0.01 | 0.98 ±0.02 | 0.99±0.01 | 0.99±0.01 |

[1] $M_h(\theta_{th})$ means $M_h$ is a function of $\theta_{th}$ (case study 1). A similar definition applies to the other cases. RMSEs and MAEs are in $[Nm/kg]$ [2] See also Fig. 6.

TABLE II
COMPARISON OF AVERAGE(±STD) RMS ERRORS, MAES AND $\rho_{cc}$ (SEE ALSO SUBSECTION III-E & III-F)

| | Database 2 | | | | Database 3 | | | |
|---|---|---|---|---|---|---|---|---|
| | $M_h(\theta_{th})$ | $M_k(\theta_{th})$ | $M_a(\theta_{th})$ | $M_a(\theta_{sh})$ | $M_h(\theta_{th})$ | $M_k(\theta_{th})$ | $M_a(\theta_{th})$ | $M_a(\theta_{sh})$ |
| RMSE | 0.13±0.03 | 0.13±0.04 | 0.12±0.06 | 0.15±0.05 | 0.10±0.03 | 0.11±0.03 | 0.10±0.03 | 0.11±0.03 |
| MAE | 0.09±0.02 | 0.09±0.02 | 0.08±0.03 | 0.10±0.02 | 0.07±0.02 | 0.07±0.02 | 0.07±0.02 | 0.07±0.02 |
| $\rho_{cc}$ | 0.94±0.03 | 0.82±0.12 | 0.97±0.04 | 0.95±0.03 | 0.94±0.04 | 0.80±0.09 | 0.97±0.02 | 0.97±0.01 |

Unlike the first database, subjects in the second and third database did not perform experiments at specific speeds, but rather the speeds were different for each participant. As a result, for these databases the results are not reported according to the speeds and it was not possible for us to show the curves in one figure, similar to what we did in Fig.7. Therefore, in the following subsections, for each quality measure (RMS errors, MAEs, $\rho_{cc}$), the mean of all of the subjects and all of the speeds are reported instead (Tab. II).

### E. RMS Errors, MAEs and $\rho_{cc}$ for Second Database [40]

*1) Estimating Hip Moment Using Thigh Angles:* The average±std RMS errors, MAEs and $\rho_{cc}$ were 0.13±0.03 [Nm/kg], 0.09±0.02 [Nm/kg] and 0.94±0.03, respectively. The size of $x(k)$ was 5, i.e., $x(k) = [u(k), \ldots, u(k-4)]$.

*2) Estimating Knee Moment Using Thigh Angles:* The average±std RMS errors, MAEs and $\rho_{cc}$ were 0.13±0.04 [Nm/kg], 0.09±0.02 [Nm/kg] and 0.82±0.12, respectively. The size of $x(k)$ was 3.

*3) Estimating Ankle Moment Using Thigh Angles:* The average±std RMS errors, MAEs and $\rho_{cc}$ were 0.12±0.06 [Nm/kg], 0.08±0.03 [Nm/kg] and 0.97±0.04, respectively. The size of $x(k)$ was 3.

*4) Estimating Ankle Moment Using Shank Angles:* The average±std RMS errors, MAEs and $\rho_{cc}$ were 0.15±0.05 [Nm/kg], 0.10±0.02 [Nm/kg] and 0.95±0.03, respectively. The size of $x(k)$ was 2.

### F. RMS Errors, MAEs and $\rho_{cc}$ for Third Database [41]

*1) Estimating Hip Moment Using Thigh Angles:* The average±std RMS errors, MAEs and $\rho_{cc}$ were 0.10±0.03 [Nm/kg], 0.07±0.02 [Nm/kg] and 0.94±0.04, respectively. The size of $x(k)$ was 4.

*2) Estimating Knee Moment Using Thigh Angles:* The average±std RMS errors, MAEs and $\rho_{cc}$ were 0.11±0.03 [Nm/kg], 0.07±0.02 [Nm/kg] and 0.80±0.09, respectively. The size of $x(k)$ was 3.

*3) Estimating Ankle Moment Using Thigh Angles:* The average±std RMS errors, MAEs and $\rho_{cc}$ were 0.10±0.03 [Nm/kg], 0.07±0.02 [Nm/kg] and 0.97±0.02, respectively. The size of $x(k)$ was 3.

*4) Estimating Ankle Moment Using Shank Angles:* The average±std RMS errors, MAEs and $\rho_{cc}$ were 0.11±0.03 [Nm/kg], 0.07±0.02 [Nm/kg] and 0.97±0.01, respectively. The size of $x(k)$ was 3. In order to better compare the results of these two databases with database 1 (Tab. I), the outcomes are also reported in Tab. II.

## IV. DISCUSSIONS & CONCLUSION

Thigh and shank angles, were used to estimate ankle, knee and hip moments in this work. Several case studies were investigated and the results were reported.

Comparing the $\rho_{cc}$ results related to the three databases (Tabs. I, II), we see some similarities between the outcomes obtained in III-C, III-E, III-F. The best results were achieved when estimating ankle moments using thigh or shank angles. The second best results were related to the hip moment estimations, and the third place belongs to knee moment estimations. This trend is commonly observable in all three databases as reported in Tabs. I and II. The weakest estimation performance was observed when knee moments were estimated using thigh angles at 0.5 m/s in Tab. I. In this case, the estimation quality was much better at 1.5 m/s.

According to the results seen in subsection III-C, Figs. 6 and 7, and Tab. I, in general, the estimation quality was lower for lower speeds. For hip and knee joints, the differences are more obvious. For ankle joint, however, the differences are very slight either for thigh or shank inputs. The lower estimation quality for the knee joint is also reported in [28] and [56]. One possible explanation could be that lower walking speed has less energy efficiency in comparison to normal walking [57]. This might possibly be linked to the relationship between kinematics and kinetics of this joint at lower speeds. This may come into more attention when we see that for this joint the input source and method was the same, however performance was better at higher speeds. On the

TABLE III
COMPARISON OF THIS STUDY WITH DIFFERENT STUDIES (SEE ALSO SECTION IV FOR MORE INFORMATION)

| Study | No. of Sources & Type of the Inputs | Algorithm | No. of Participants | Walk. Speeds | Ave. (N)RMSE $\frac{Nm}{kg}$ | Ave. (N)MAE $\frac{Nm}{kg}$ | Ave. $\rho_{cc}$ or $R^2$ |
|---|---|---|---|---|---|---|---|
| [28] (Hip Mom.) | 12\| Demog., Anthropo., Kine., EMG | feed-forward NN | 19 | self-selected | 0.2 | — | $R^2$: 0.88 – 0.90 |
| (Kne. Mom.) | 12 \| see above | | | | 0.08 – 0.10 | — | $R^2$: 0.82 – 0.90 |
| (Ank. Mom.) | 10 \| see above | | | | 0.10 – 0.12 | — | $R^2$: 0.95 – 0.97 |
| [28] (Hip Mom.) | 3 \| $\ddot{\theta}_h$ , $\dot{\theta}_h$ , $\theta_h$ | feed-forward NN | 19 | self-selected | — | — | $R^2$: 0.93 |
| (Kne. Mom.) | 3 \| $\ddot{\theta}_k$ , $\dot{\theta}_k$ , $\theta_k$ | | | | — | — | $R^2$: 0.70 |
| (Ank. Mom.) | 3 \| $\ddot{\theta}_a$ , $\dot{\theta}_a$ , $\theta_a$ | | | | — | — | $R^2$: 0.96 |
| [29] (Hip Mom.) | 7 \| joint ang., height, weight, & speed, thigh/shank/foot length | LSTM with recurrent NN | 12 | 0.8 – 2.0 | 2 – 18 % (N) | — | — |
| (Kne Mom.) | | | | | 2 – 13 % | — | — |
| (Ank. Mom.) | | | | | 1 – 6 % | — | — |
| [33] (Hip Mom.) | 3 \| $\theta_h$ , $\theta_k$ , $\theta_a$ | ANN | 2 | self-selected | 0.17 – 0.67 | — | — |
| [22] (Ank. Mom.) | 2 \| EMG | ANN | 40 | one test speed | 0.04 | — | 0.99 |
| [17] (Hip Mom.) | 35 \| $\theta_h$ , acc. & ang. vel. | XGBoost | 5 | self-selected | 0.09 | — | — |
| [30] (Hip Mom.) | 18 \| lin. acc. & ang.vel. of thigh, shank, foot | LSTM | not avail. | 0.8 – 2.0 | 9.8% (N) | — | 0.98 (stance phase) |
| (Kne. Mom.) | | | | | 11.8% (N) | — | 0.96 (stance phase) |
| (Ank. Mom.) | | | | | 7.3% (N) | — | 0.98 (stance phase) |
| [30] (Hip Mom.) | 18 \| lin. acc. & ang.vel. of thigh, shank, foot | FFNN | not avail. | 0.8 – 2.0 | 10.2% (N) | — | 0.98 (stance phase) |
| (Kne. Mom.) | | | | | 9.4% (N) | — | 0.98 (stance phase) |
| (Ank. Mom.) | | | | | 7.3% (N) | — | 0.99 (stance phase) |
| [21] (Kne. Mom.) | 14 \| $\theta_k$ & EMG | EMG-driven model | 6 | run. 3 m/s | — | 0.13 – 0.19 | $R^2$: 0.86 - 0.93 |
| [56] (Hip Mom.) | 16 \| EMG | CEINMS | 5 | 1.5 | 0.39 | — | $R^2$: 0.84 |
| (Kne. Mom.) | | | | | 0.18 | — | $R^2$: 0.80 |
| (Ank. Mom.) | | | | | 0.24 | — | $R^2$: 0.88 |
| [20] (Hip Mom.) | 16 \| EMG | EMG-driven forward-dynamics | 1 | 1.3 | — | 10 – 15 % (N) | — |
| (Kne. Mom.) | | | | | — | 14 % (N) | — |
| (Ank. Mom.) | | | | | — | 9 – 11 % (N) | — |
| [59] (Hip Mom.) | 52 \| body attached markers | inverse dynamics based only on kinematics | 3 | 1.5, 1.9 | 0.46 – 0.61 | — | — |
| (Kne. Mom.) | | | | | 0.30 – 0.37 | — | — |
| (Ank. Mom.) | | | | | 0.19 – 0.23 | — | — |
| [31] (Ank. Mom.) | 1 \| $\theta_a$<br>1 \| Achill. ten. force<br>10 \| $\theta_a$ , Ach. forc. & eight bladders in insole | ANN | 6 | 1.0, 1.5 | 15 – 16 % (N)<br>20 – 23 % (N)<br>6 – 7 % (N) | — | — |
| This study (Hip Mom.) | 1 \| $\theta_{th}$ | NARX with wavelets | 21 (first database [39]) | 0.5, 1, 1.5 | 0.13 – 0.15 | 0.10 – 0.11 | 0.90 – 0.98 |
| (Kne. Mom.) | 1 \| $\theta_{th}$ | | | | 0.13 | 0.09 – 0.10 | 0.71 – 0.96 |
| (Ank. Mom.) | 1 \| $\theta_{th}$ | | | | 0.10 – 0.13 | 0.07 – 0.10 | 0.96 – 0.98 |
| (Ank. Mom.) | 1 \| $\theta_{sh}$ | | | | 0.09 – 0.12 | 0.06 – 0.08 | 0.98 – 0.99 |

(N) denotes Normalized values, presented in percent [%].
LSTM: Long Short Term Memory
CEINMS: Calibrated EMG-Informed Neuro-Musculo-Skeletal Modeling

other side, the results of the ankle joint are not supporting the above statement, where even for lower speed, good results were obtained. Nevertheless, if and how kinetics, kinematics, and gait energetics could be correlated and impact the estimation accuracy requires further in-depth investigations. Another explanation could be that the number of input sources or type of the inputs, or even the processing algorithm was not suitable for that specific speed. The results might get improved if, e.g., the inputs were combined with angular velocities and/or EMG signals. However, Tab. III shows that even with high number of inputs, some studies have reported the lowest $R^2$ values for this joint [28], [56]. Furthermore, in [15] we showed that a Gaussian process regression fed only by shank angles or only angular velocities did not lead to acceptable ankle moment estimation, however in this study shank angles were sufficient using the proposed algorithm. The above discussions can form starting points for further investigations.

The performance of the estimator was investigated as well when past estimated outputs $[y(k-1), y(k-2), \ldots]$ were included in the input $x(k)$ (see Fig. 3). Here, the results are reported for two case studies with data from the second database [40]. The average values are the mean of all of the subjects and speeds. For hip moment estimations using thigh angles, when $x(k) = [u(k), \ldots, u(k-4), y(k-1)]$, the average RMS errors, MAEs and $\rho_{cc}$ were 0.35 Nm/kg, 0.29 Nm/kg, and 0.87, respectively. In this case, further investigation showed that when $x(k) = [u(k), \ldots, u(k-4), y(k-1), y(k-2)]$, the average values were 0.18, 0.13, and 0.91, respectively. For ankle moment estimations using shank angles, when $x(k) = [u(k), \ldots, u(k-4), y(k-1)]$, the average RMS errors, MAEs and $\rho_{cc}$ were 0.43 Nm/kg, 0.28 Nm/kg, and 0.78, respectively.

Compared with the results seen in subsections III-E.1 and III-E.4 (where past outputs of $y$ were not included), the inclusion of the previous outputs $y$ in the $x(k)$ does not necessarily lead to better estimation performance. This point can potentially reduce the computation time required by the algorithm.

The impact of different training approaches on the estimation quality was investigated as well. Here the results are reported for two case studies when hip moments were estimated using thigh angles. Using first database [39], in the first case study, the inputs from the first two lowest speeds were used for training, and the input from all of the speeds was used for testing. The average±std RMS errors were 0.12±0.05, 0.13±0.05 and 0.25±0.10 [Nm/kg]. For MAEs the

values were 0.14±0.06, 0.08±0.03, 0.11±0.04 [Nm/kg] and for $\rho_{cc}$ the values were 0.92±0.07, 0.97±0.02, 0.91±0.05, for 0.5, 1 and 1.5 m/s respectively.

Next, for the second case study, inputs from the lowest and highest speeds were used for training, and the input from all of the speeds was used for testing. The average±std RMS errors were 0.12±0.05, 0.14±0.05 and 0.15±0.05 [Nm/kg], the average±std MAEs were 0.15±0.07, 0.09±0.03, 0.07±0.02 [Nm/kg] and the average±std $\rho_{cc}$ were 0.90±0.09, 0.96±0.03, 0.98±0.01, for 0.5, 1 and 1.5 m/s respectively.

A similar procedure was done for the second database [40] as well as the third one. At first, the input from the first two lowest speeds was used for training, and the input from the remaining six speeds was used for testing. The average±std RMS errors, MAEs and $\rho_{cc}$ were 0.26±0.05 [Nm/kg], 0.19±0.04 [Nm/kg] and 0.80±0.09, respectively (average of all of the subjects and all of the speeds).

Next, the input from the lowest and highest speeds was used for training, and the input from the remaining six speeds was used for testing. The average±std RMS errors, MAEs and $\rho_{cc}$ were 0.19±0.07 [Nm/kg], 0.14±0.05 [Nm/kg] and 0.90±0.05, respectively.

Similarly, for the third database [41], in the first case, the average±std RMS errors, MAEs and $\rho_{cc}$ were 0.17±0.09 [Nm/kg], 0.13±0.06 [Nm/kg] and 0.88±0.07, respectively (average of all of the subjects and all of the speeds). For the second case, the average±std RMS errors, MAEs and $\rho_{cc}$ were 0.14±0.10 [Nm/kg], 0.11±0.08 [Nm/kg] and 0.89±0.11, respectively (average of all of the subjects and all of the speeds).

According to the results obtained, the estimation performance was better (in some cases slightly) in interpolation (second case study) than extrapolation (first case study). This finding can be potentially used for planning relatively efficient and less time-consuming training procedures. In this regard, at first the data at the lower and upper boundary conditions can be used for training, and then the estimation quality of the algorithm can be evaluated. Next, the results can be compared with those of a full-data training.

This finding was similar to what we saw in our previous studies, in which the estimation results for interpolation approach and for full-data training were relatively similar [34], [58]. Further future studies can better reveal the pros and cons of such a training approach for various locomotion modes.

A number of studies have suggested different methods to estimate ankle, knee or hip moments. In those works, different algorithms and inputs were proposed and used, and the approaches were verified on different number of participants. Tab. III presents a summary of the results obtained from several studies in this regard. It also compares them with the results obtained in this study. The table shows that both mechanical (kinetics, kinematics) and EMG signals were used to estimate the moments, depending on the algorithm. Furthermore, biometric data such as age and height were used in a number of studies as well, e.g., [28], [29]. In this work, we used one source of input for each case study (shank angles or thigh angles, see Methods section). The table shows the obtained results are comparable to different studies. Interestingly, a part of our findings was similar to what other researchers have reported in different studies. For instance, [28], [56], reported better $R^2$ results for ankle and hip joints in comparison to knee joint. The results reported by [30], show much better results for the knee joint, however, they have benefited from eighteen different signals into their algorithm. We reached a relatively similar result at higher speed (1.5 m/s), using only one input signal. Study [17] reports relatively better results for the hip joint in comparison to ours, however the number of the inputs are considerably higher than our work. Furthermore, the number of the studied participants is much less than this study. The table also shows that the vast majority of the studies have used mechanical or EMG signals.

In addition to the above, our study has a main difference with some of the studies above. As an example, [31] uses the ankle angle to estimate the ankle moment. Although this method is very useful for human gait studies, it is not appropriate for controlling a foot prosthesis, because in this situation there is no biological limb whose inputs could be used into the controller. Our method, in contrary, proposes to use a lower limb above the specific joint, and therefore avoids this problem. This is one of the fundamental differences between our approach and the approaches used by most of the studies in Tab. III. In addition, since the motion of the lower limbs is mainly governed by the central nervous system, the inputs originating from them would result in a more robust and reliable motion planner.

This work aimed to create connection between the motion of shank or thigh and the moments of ankle, knee and hip. A main challenge in design of smart exoskeletons, orthoses or prostheses is developing a controller that can generate human-like motions at the joints level. The generated motions should be in line with those of the remaining biological limbs. The estimation approach presented in this work can be potentially used in designing high-level controllers and motion planners for orthotics, exoskeletons, prosthetics, and humanoids. The inputs to the algorithm can be obtained from thigh- or shank-mounted IMUs (inertial measurement units) which is a common approach in this field, e.g., see [1], [60]. Next, the inputs are fed into the motion planner to estimate the joint moment corresponding to the lower limb angle. Using a laptop equipped with 16 GB RAM and Intel Core i7 CPU, the computation time was less than 1 $msec$ for a one-to-one estimation. This time is relatively good enough considering the working condition of current orthotic/prosthetic devices (e.g., 1 kHz in [6] and [60]). When a desired estimated value is generated, using e.g., a PD controller, a corresponding error signal is produced. Next, using controller gains, appropriate command signal can be sent to the actuator (motor). In this way, the actuator operation will be a function of the lower limb motion.

The proposed method is specially useful when a device is equipped with springs. Since in this situation the motion of the joint gets decoupled from the motion of the actuator (motor), having information about the required moment (force) will be vital in order to estimate the desired position of the

actuator. In this case, the current study can be combined with our previous study presented in [34], in order to estimate the corresponding position of the actuator. Further information on how to use moment and angle estimation in order to estimate the corresponding actuator position can be found in [57].

In this work, able-bodied gait data was used to analyze the estimation results. One logical approach in designing motion planners for assistive devices is to identify the rules or the relationships latent in healthy human locomotion. These relationships can act as a target frame and possibly gold standard for the behavior of a powered prosthetic or orthotic device. The performance of these devices can then be tailored to meet individual requirements. Therefore, to create a target frame for device's performance, decoding the latent relationships in average able-bodied human gait is a necessary pre-requisite. In this study, we showed that relationships exist between the motions of a limb and the moment generated in a (corresponding) joint. The identified relationships can be used as potential guidelines to bring and keep the performance of a prosthesis or orthosis within a biomechanically logical region (in terms of kinematics and kinetics).

In case of the amputees, those input data should inevitably come from the remaining lower limbs. One logical thinking is that if the inputs from this population are similar to those of able-bodied participants we used in this study, the corresponding outputs should be in a similar region. Therefore, we decided to compare the similarities between the amputee inputs and able-bodied inputs. To do so, transfemoral amputee data released publicly by [61] was used. Next, thigh angles were extracted by a Matlab program and compared with the average able-bodied subjects obtained from the first database [39]. The results showed that for slow, moderate and fast walking speeds, the correlation coefficients were 0.93 – 0.99, 0.95 – 0.99, and 0.93 – 0.98 for ten amputees (23 – 65 yrs old) [34]. These values show that the inputs from the two groups have sufficient correspondence. Therefore, for these amputees, thigh angles can be potentially used to estimate the corresponding required ankle or knee moments if a robotic prosthesis is going to be used. Since the number of the amputees were limited, further clinical experiments with bigger groups of amputees would be required to analyze and compare more thoroughly the similarities and differences of the inputs.

In this study, sagittal plane joints' moments were estimated during walking gait. In order to have a more comprehensive algorithm, one direction of the future work can be to investigate the functionality of the presented estimation method for other locomotion types such as descending or ascending the slopes or stairs. In addition, the work can be continued to investigate the estimation performance for other anatomical planes.

## Acknowledgment

In this study the authors used gait data from three different publications [39], [40], and [41]. Hereby, they would like to express our gratitude to those authors for sharing their data.

## References

[1] M. A. Holgate, T. G. Sugar, and A. W. Bohler, "A novel control algorithm for wearable robotics using phase plane invariants," in *Proc. IEEE Int. Conf. Robot. Autom. (ICRA)*, May 2009, pp. 3845–3850.
[2] F. Sup, A. Bohara, and M. Goldfarb, "Design and control of a powered transfemoral prosthesis," *Int. J. Robot. Res.*, vol. 27, no. 2, pp. 263–273, Feb. 2008.
[3] H. A. Varol, F. Sup, and M. Goldfarb, "Multiclass real-time intent recognition of a powered lower limb prosthesis," *IEEE Trans. Biomed. Eng.*, vol. 57, no. 3, pp. 542–551, Mar. 2010.
[4] F. Sup, H. A. Varol, and M. Goldfarb, "Upslope walking with a powered knee and ankle prosthesis: Initial results with an amputee subject," *IEEE Trans. Neural Syst. Rehabil. Eng.*, vol. 19, no. 1, pp. 71–78, Feb. 2011.
[5] R. Riener, L. Lünenburger, I. Maier, G. Colombo, and V. Dietz, "Locomotor training in subjects with sensori-motor deficits: An overview of the robotic gait orthosis lokomat," *J. Healthcare Eng.*, vol. 1, no. 2, pp. 197–216, Jun. 2010.
[6] J. Ward, T. Sugar, A. Boehler, J. Standeven, and J. R. Engsberg, "Stroke survivors' gait adaptations to a powered ankle–foot orthosis," *Adv. Robot.*, vol. 25, no. 15, pp. 1879–1901, Jan. 2011.
[7] S. Culver, H. Bartlett, A. Shultz, and M. Goldfarb, "A stair ascent and descent controller for a powered ankle prosthesis," *IEEE Trans. Neural Syst. Rehabil. Eng.*, vol. 26, no. 5, pp. 993–1002, May 2018.
[8] S. Maggioni, N. Reinert, L. Lünenburger, and A. Melendez-Calderon, "An adaptive and hybrid end-point/joint impedance controller for lower limb exoskeletons," *Frontiers Robot. AI*, vol. 5, p. 104, Oct. 2018.
[9] G. A. Ribeiro, L. N. Knop, and M. Rastgaar, "Multi-directional ankle impedance during standing postures," *IEEE Trans. Neural Syst. Rehabil. Eng.*, vol. 28, no. 10, pp. 2224–2235, Oct. 2020.
[10] D. A. Winter, *Biomechanics and Motor Control of Human Movement*. Hoboken, NJ, USA: Wiley, 2009.
[11] E. J. Rouse, L. M. Mooney, and H. M. Herr, "Clutchable series-elastic actuator: Implications for prosthetic knee design," *Int. J. Robot. Res.*, vol. 33, no. 13, pp. 1611–1625, 2014.
[12] A. H. Shultz, J. E. Mitchell, D. Truex, B. E. Lawson, E. Ledoux, and M. Goldfarb, "A walking controller for a powered ankle prosthesis," in *Proc. 36th Annu. Int. Conf. IEEE Eng. Med. Biol. Soc.*, Aug. 2014, pp. 6203–6206.
[13] E. S. Altinkaynak and D. J. Braun, "A phase-invariant linear torque-angle-velocity relation hidden in human walking data," *IEEE Trans. Neural Syst. Rehabil. Eng.*, vol. 27, no. 4, pp. 702–711, Apr. 2019.
[14] T. G. Sugar, S. Redkar, and K. W. Hollander, "Phase controller outperforms impedance controller for a hip exoskeleton," *MOJ Appl. Bionics Biomech.*, vol. 4, no. 1, pp. 25–28, 2020. [Online]. Available: https://medcraveonline.com/MOJABB/phase-controller-outperforms-impedance-controller-for-a-hip-exoskeleton.html
[15] M. Eslamy and K. Alipour, "Synergy-based Gaussian process estimation of ankle angle and torque: Conceptualization for high level controlling of active robotic foot prostheses/othoses," *J. Biomech. Eng.*, vol. 141, no. 2, Feb. 2019, Art. no. 021002.
[16] I. Kang, P. Kunapuli, and A. J. Young, "Real-time neural network-based gait phase estimation using a robotic hip exoskeleton," *IEEE Trans. Med. Robot. Bionics*, vol. 2, no. 1, pp. 28–37, Feb. 2020.
[17] D. D. Molinaro, I. Kang, J. Camargo, and A. J. Young, "Biological hip torque estimation using a robotic hip exoskeleton," in *Proc. 8th IEEE RAS/EMBS Int. Conf. Biomed. Robot. Biomechatronics (BioRob)*, Nov. 2020, pp. 791–796.
[18] F. Sepulveda, D. M. Wells, and C. L. Vaughan, "A neural network representation of electromyography and joint dynamics in human gait," *J. Biomech.*, vol. 26, no. 2, pp. 101–109, Feb. 1993.
[19] R. A. Bogey and L. A. Barnes, "An EMG-to-force processing approach for estimating in vivo hip muscle forces in normal human walking," *IEEE Trans. Neural Syst. Rehabil. Eng.*, vol. 25, no. 8, pp. 1172–1179, Aug. 2017.
[20] M. Sartori, M. Reggiani, D. Farina, and D. G. Lloyd, "EMG-driven forward-dynamic estimation of muscle force and joint moment about multiple degrees of freedom in the human lower extremity," *PLoS ONE*, vol. 7, no. 12, Dec. 2012, Art. no. e52618.
[21] D. G. Lloyd and T. F. Besier, "An EMG-driven musculoskeletal model to estimate muscle forces and knee joint moments in vivo," *J. Biomech.*, vol. 36, no. 6, pp. 765–776, Jun. 2003.
[22] A. D. Keleş and C. A. Yucesoy, "Development of a neural network based control algorithm for powered ankle prosthesis," *J. Biomech.*, vol. 113, Dec. 2020, Art. no. 110087.
[23] M. M. Ardestani et al., "Human lower extremity joint moment prediction: A wavelet neural network approach," *Expert Syst. Appl.*, vol. 41, no. 9, pp. 4422–4433, Jul. 2014.

[24] H. Huang, F. Zhang, L. J. Hargrove, Z. Dou, D. R. Rogers, and K. B. Englehart, "Continuous locomotion-mode identification for prosthetic legs based on neuromuscular–mechanical fusion," *IEEE Trans. Biomed. Eng.*, vol. 58, no. 10, pp. 2867–2875, Oct. 2011.

[25] R. Gupta, I. S. Dhindsa, and R. Agarwal, "Continuous angular position estimation of human ankle during unconstrained locomotion," *Biomed. Signal Process. Control*, vol. 60, Jul. 2020, Art. no. 101968.

[26] A. J. Young, T. A. Kuiken, and L. J. Hargrove, "Analysis of using EMG and mechanical sensors to enhance intent recognition in powered lower limb prostheses," *J. Neural Eng.*, vol. 11, no. 5, Oct. 2014, Art. no. 056021.

[27] Y. Li, Q. Zhang, N. Zeng, M. Du, and Q. Zhang, "Prediction of knee joint moment by surface electromyography of the antagonistic and agonistic muscle pairs," *IEEE Access*, vol. 7, pp. 82320–82328, 2019.

[28] M. E. Hahn and K. B. O'Keefe, "A neural network model for estimation of net joint moments during normal gait," *J. Musculoskeletal Res.*, vol. 11, no. 3, pp. 117–126, Sep. 2008.

[29] M. Mundt, A. Koeppe, F. Bamer, W. Potthast, and B. Markert, "Prediction of joint kinetics based on joint kinematics using neural networks," in *Proc. 36th Conf. Int. Soc. Biomech. Sports*, Auckland, New Zealand, 2018, pp. 794–797.

[30] M. Marion et al., "Prediction of lower limb joint angles and moments during gait using artificial neural networks," *Med. Biol. Eng. Comput.*, vol. 58, no. 16, pp. 211–225, 2020.

[31] D. A. Jacobs and D. P. Ferris, "Estimation of ground reaction forces and ankle moment with multiple, low-cost sensors," *J. NeuroEng. Rehabil.*, vol. 12, no. 1, pp. 1–12, Dec. 2015.

[32] G. Khademi and D. Simon, "Toward minimal-sensing locomotion mode recognition for a powered knee-ankle prosthesis," *IEEE Trans. Biomed. Eng.*, vol. 68, no. 3, pp. 967–979, Mar. 2021.

[33] P. Osateerakun, G. Barton, R. Foster, S. Bennett, and R. Lakshminarayan, "P 037—Prediction of moments from movements without force platforms using artificial neural networks: A pilot test," *Gait Posture*, vol. 65, pp. 299–300, Sep. 2018.

[34] M. Eslamy and A. F. Schilling, "Estimation of knee and ankle angles during walking using thigh and shank angles," *Bioinspiration Biomimetics*, vol. 16, no. 6, Nov. 2021, Art. no. 066012.

[35] I. Daubechies, *Ten Lectures on Wavelets*. Philadelphia, PA, USA: SIAM, 1992.

[36] I. Daubechies, "The wavelet transform, time-frequency localization and signal analysis," *IEEE Trans. Inf. Theory*, vol. 36, no. 5, pp. 961–1005, Sep. 1990.

[37] S. G. Mallat, "A theory for multiresolution signal decomposition: The wavelet representation," *IEEE Trans. Pattern Anal. Mach. Intell.*, vol. 11, no. 7, pp. 674–693, Jul. 1989.

[38] I. Daubechies, "Orthonormal bases of compactly supported wavelets," *Commun. Pure Appl. Math.*, vol. 41, no. 7, pp. 909–996, 1988.

[39] S. Lipfert, *Kinematic and Dynamic Similarities Between Walking and Running*. Hamburg, Germany: Verlag Dr. Kovac, 2010.

[40] C. A. Fukuchi, R. K. Fukuchi, and M. Duarte, "A public dataset of overground and treadmill walking kinematics and kinetics in healthy individuals," *PeerJ*, vol. 6, Apr. 2018, Art. no. e4640.

[41] T. Lencioni, I. Carpinella, M. Rabuffetti, A. Marzegan, and M. Ferrarin, "Human kinematic, kinetic and EMG data during different walking and stair ascending and descending tasks," *Sci. Data*, vol. 6, no. 1, pp. 1–10, Dec. 2019.

[42] R. Isermann and M. Münchhof, *Identification of Dynamic Systems: An Introduction With Applications*. Heidelberg, Germany: Springer-Verlag, 2010.

[43] S. Farmer, B. Silver-Thorn, P. Voglewede, and S. A. Beardsley, "Within-socket myoelectric prediction of continuous ankle kinematics for control of a powered transtibial prosthesis," *J. Neural Eng.*, vol. 11, no. 5, 2014, Art. no. 056027.

[44] T. Lin, B. G. Horne, P. Tiňo, and C. L. Giles, "Learning long-term dependencies in NARX recurrent neural networks," *IEEE Trans. Neural Netw.*, vol. 7, no. 6, pp. 1329–1338, Nov. 1996.

[45] Z. Boussaada, O. Curea, A. Remaci, H. Camblong, and N. M. Bellaaj, "A nonlinear autoregressive exogenous (NARX) neural network model for the prediction of the daily direct solar radiation," *Energies*, vol. 11, no. 3, p. 620, Mar. 2018.

[46] Q. Zhang, "Using wavelet network in nonparametric estimation," *IEEE Trans. Neural Netw.*, vol. 8, no. 2, pp. 227–236, Mar. 1997.

[47] Q. Zhang and A. Benveniste, "Wavelet networks," *IEEE Trans. Neural Netw.*, vol. 3, no. 6, pp. 889–898, Nov. 1992.

[48] T. Kugarajah and Q. Zhang, "Multidimensional wavelet frames," *IEEE Trans. Neural Netw.*, vol. 6, no. 6, pp. 1552–1556, Nov. 1995.

[49] S. Chen, C. F. N. Cowan, and P. M. Grant, "Orthogonal least squares learning algorithm for radial basis function networks," *IEEE Trans. Neural Netw.*, vol. 2, no. 2, pp. 302–309, Mar. 1991.

[50] D. Popovic and S. Jonic, "Determining synergy between joint angles during locomotion by radial basis function neural networks," in *Proc. IEEE Eng. Med. Biol. Soc.*, vol. 5, Nov. 1998, pp. 2301–2304.

[51] S. Jonic, T. Jankovic, V. Gajic, and D. Popvic, "Three machine learning techniques for automatic determination of rules to control locomotion," *IEEE Trans. Biomed. Eng.*, vol. 46, no. 3, pp. 300–310, Mar. 1999.

[52] I. Milovanovic, "Radial basis function (RBF) networks for improved gait analysis," in *Proc. 9th Symp. Neural Netw. Appl. Electr. Eng.*, Sep. 2008, pp. 129–132.

[53] M. Thor, T. Kulvicius, and P. Manoonpong, "Generic neural locomotion control framework for legged robots," *IEEE Trans. Neural Netw. Learn. Syst.*, vol. 32, no. 9, pp. 4013–4025, Sep. 2021.

[54] J. Y. Goulermas, D. Howard, C. J. Nester, R. K. Jones, and L. Ren, "Regression techniques for the prediction of lower limb kinematics," *J. Biomech. Eng.*, vol. 127, no. 6, pp. 1020–1024, Nov. 2005.

[55] A. Findlow, J. Goulermas, C. Nester, D. Howard, and L. Kenney, "Predicting lower limb joint kinematics using wearable motion sensors," *Gait Posture*, vol. 28, no. 1, pp. 120–126, 2008.

[56] C. Pizzolato et al., "CEINMS: A toolbox to investigate the influence of different neural control solutions on the prediction of muscle excitation and joint moments during dynamic motor tasks," *J. Biomech.*, vol. 48, no. 14, pp. 3929–3936, Nov. 2015.

[57] M. Eslamy, "Emulation of ankle function for different gaits through active foot prosthesis: Actuation concepts, control and experiments," Ph.D. dissertation, Dept. Mech. Eng., Technische Universität Darmstadt, Darmstadt, Germany, 2014.

[58] M. Eslamy, F. Oswald, and A. Schilling, "Mapping thigh motion to knee motion: Implications for motion planning of active prosthetic knees," in *Proc. IEEE/RSJ Int. Conf. Intell. Robots Syst. (IROS)*, Oct. 2020, pp. 4120–4125.

[59] L. Ren, R. K. Jones, and D. Howard, "Whole body inverse dynamics over a complete gait cycle based only on measured kinematics," *J. Biomech.*, vol. 41, no. 12, pp. 2750–2759, 2008.

[60] D. Quintero, D. J. Villarreal, D. J. Lambert, S. Kapp, and R. D. Gregg, "Continuous-phase control of a powered knee–ankle prosthesis: Amputee experiments across speeds and inclines," *IEEE Trans. Robot.*, vol. 34, no. 3, pp. 686–701, Jun. 2018.

[61] S. Hood, M. K. Ishmael, A. Gunnell, K. B. Foreman, and T. Lenzi, "A kinematic and kinetic dataset of 18 above-knee amputees walking at various speeds," *Scientific Data*, vol. 7, no. 1, pp. 1–8, May 2020.